Highly pathogenic H5N1 influenza virus can enter the central nervous system and induce neuroinflammation and neurodegeneration

Haeman Jang[a,b], David Boltz[c], Katharine Sturm-Ramirez[c,1], Kennie R. Shepherd[a,2], Yun Jiao[a], Robert Webster[c], and Richard J. Smeyne[a,3]

Departments of [a]Developmental Neurobiology and [c]Infectious Diseases/Virology, St. Jude Children's Research Hospital, 262 Danny Thomas Place, Memphis, TN 38105-3678; and [b]Integrated Program in Biomedical Sciences, University of Tennessee Health Science Center, Memphis, TN 38163

Edited by Floyd E. Bloom, The Scripps Research Institute, La Jolla, CA, and approved June 30, 2009 (received for review January 8, 2009)

One of the greatest influenza pandemic threats at this time is posed by the highly pathogenic H5N1 avian influenza viruses. To date, 61% of the 433 known human cases of H5N1 infection have proved fatal. Animals infected by H5N1 viruses have demonstrated acute neurological signs ranging from mild encephalitis to motor disturbances to coma. However, no studies have examined the longer-term neurologic consequences of H5N1 infection among surviving hosts. Using the C57BL/6J mouse, a mouse strain that can be infected by the A/Vietnam/1203/04 H5N1 virus without adaptation, we show that this virus travels from the peripheral nervous system into the CNS to higher levels of the neuroaxis. In regions infected by H5N1 virus, we observe activation of microglia and alpha-synuclein phosphorylation and aggregation that persists long after resolution of the infection. We also observe a significant loss of dopaminergic neurons in the substantia nigra pars compacta 60 days after infection. Our results suggest that a pandemic H5N1 pathogen, or other neurotropic influenza virus, could initiate CNS disorders of protein aggregation including Parkinson's and Alzheimer's diseases.

alpha-synuclein | Parkinson's disease | substantia nigra | stereology | encephalitis

At this time, one of the greatest worldwide pandemic threats is posed by the highly pathogenic H5N1 family of avian influenza A viruses; where to date, 61% of the 433 known human cases of H5N1 infection have proved fatal (1). Although most infections primarily affect the respiratory system, neurological symptoms have been associated with past influenza type A outbreaks, including the 1918 "Spanish" influenza pandemic (2, 3). In recent times, poultry (4) and humans (5, 6) infected by H5N1 have shown acute neurological signs ranging from mild encephalitis to motor disturbances to coma. However, despite these acute descriptions, no studies have examined the longer-term neurologic consequences of H5N1 infection in surviving hosts.

It has been hypothesized that viruses have an etiological role in the development of several neurodegenerative disorders including the two most common, Alzheimer's and Parkinson's diseases (7). Each of these disorders are characterized by neuronal loss, abnormal protein aggregations (proteinopathies), and activation of the microglia that act as the brain's innate immune system (8). Parkinson's disease (PD) is characterized by a loss of the pigmented cells located in the midbrain's substantia nigra pars compacta (SNpc), although cell loss has also been described in the locus coeruleus (9), the dorsal motor nucleus of the vagus nerve (10), and throughout the autonomic nervous system (11). In addition to neuronal loss, primary PD is also defined by the presence of proteinaceous inclusion bodies called Lewy bodies. Lewy bodies were first described and linked to PD by Frederic Lewy (12), and subsequently these have been shown to consist of a number of proteins including aggregated alpha-synuclein (13). Alzheimer's disease is characterized by a general neuronal loss, neurofibrillary tangles, and abnormal deposition of proteins into cerebral plaques that are composed in part by beta-amyloid and alpha-synuclein. In this study, we directly tested whether the highly pathogenic A/VN/1204/04 H5N1 influenza virus could induce a neuronal pathology similar to that seen in proteinopathies.

Results

We first determined the infectivity of the highly pathogenic and neurotropic A/Vietnam/1203/04 (H5N1) virus by intranasally inoculating 225 6- to 8-week-old C57BL/6J mice (Jackson Laboratories) with the 50% mouse lethal dose (MLD_{50}) (14). Three days postinoculation (p.i.), approximately two-thirds of the mice demonstrated weight loss; by day 8 p.i., weight loss was >10% of initial body weight. All of the infected animals that showed weight loss showed neurological signs including ataxia, tremor, and bradykinesia. For approximately half of these animals, their symptoms became so severe that they had to be euthanized. The remainder showed milder neurological signs and recovered by day 21 p.i.

The neurological signs observed in the infected mice suggested involvement at several levels of the neuraxis. We mapped the progression of the H5N1 virus through the nervous system by using immunohistochemistry with an antibody to the influenza virus nucleoprotein (NP) (Table 1). H5N1 virus was first detected 2–3 days p.i. in the mesenteric and myenteric (Auerbach's) plexi of the enteric nervous system (Fig. 1*A*) and in neurons within the dorsal root ganglia (DRG) (Fig. 1*B*) of the peripheral nervous system. H5N1 virus was first observed in the CNS on day 3 p.i. in the brainstem solitary nucleus (Fig. 1*C*), which receives primary afferent signals from various visceral regions and organs, including lung and gut (15). On day 7 p.i., virus was found in the vagal and hypoglossal brainstem nuclei and in the midbrain locus coeruleus and SNpc (Fig, 1*D*). Outside of the brainstem and midbrain, H5N1 virus was detected in the periglomerular (Fig. 1*E*) and mitral (Fig. 1*F*) cells of the olfactory bulb and in neurons within the spinal cord (principally in the thoracic region) (Fig. 1*G*). On day 10 p.i., H5N1 infection had spread to all levels of the central neuraxis but did not involve all structures (Table 1, Fig. S1, and Fig. S2). By day 21, surviving animals

Author contributions: H.J., D.B., K.S.-R., K.R.S., R.W., and R.J.S. designed research; H.J., D.B., K.S.-R., and Y.J. performed research; H.J., D.B., K.S.-R., and R.J.S. analyzed data; and R.W. and R.J.S. wrote the paper.

The authors declare no conflict of interest.

This article is a PNAS Direct Submission.

Freely available online through the PNAS open access option.

[1]Present address: Fogarty International Center, National Institutes of Health, 16 Center Drive, Room 202, Bethesda, MD 20892.

[2]Present address: Department of Environmental and Occupational Health, Rollins School of Public Health and Center for Neurodegenerative Disease, Emory University, Whitehead Biomedical Research Building, 5th Floor, Room 575.1, Atlanta, GA, 30322.

[3]To whom correspondence should be addressed. E-mail: richard.smeyne@stjude.org.

This article contains supporting information online at www.pnas.org/cgi/content/full/0900096106/DCSupplemental.

NEUROSCIENCE

Table 1. Semi-quantitative analysis of H5N1 expression in CNS and lung

Days p.i.	Lung	Ctx	OB	DRG	Thal	SN	LC	RN	Vest n	Pons	Solitary n	VII	X	XII
1	+	-	-	ND	-	-	-	-	-	-	-	-	-	-
2	+	-	-	ND	-	-	-	-	-	-	-	-	-	-
3	++	-	-	+	-	-	-	-	-	-	+	-	-	-
7	++	-	+	ND	-	+	+	-	+	-	++	-	++	++
10	+	++	++	++	++	++	++	+	++	++	+++	++	++	+++
21	-	-	-	ND	-	-	-	-	-	-	-	-	-	-
90	-	-	-	ND	-	-	-	-	-	-	-	-	-	-

Semiquantitative immunohistochemical measurement of the percentage of anti-NP-positive cells at the indicated days p.i. with H5N1 virus. + = 0%–33%, ++ = 34%–67%, +++ = 67–100%,– = none, ND = not determined. Ctx, cerebral cortex; OB, olfactory bulb; DRG, dorsal root ganglia; Thal, thalamus; SN, SNpc; LC, locus coeruleus; RN, red nucleus; Vest n, vestibular nucleus; solitary n, solitary nucleus; VII, facial nucleus; X, vagal nucleus; XII, hypoglossal nucleus.

displayed no visible neurological signs and H5N1 virus was not detected in the CNS. The pattern of infection in lung and brain suggested that active infection lasted ≈10 days, as described in humans (5). Additional images showing the pattern of infection are shown in Fig. S1.

In the CNS, the virus was detected in neurons (Fig. 1*H*) and microglia (Fig. 1*I*) but was not seen in astrocytes (Fig. 1*J*). The presence of virus in brainstem neurons was confirmed by transmission electron microscopy, which revealed structures of the shape and size characteristic of H5N1 influenza virus (16) in the cytoplasm (Fig. 1*K*), axoplasm (Fig. 1*L*), and nucleus.

Our observation of H5N1 virus first in the enteric and peripheral nervous systems and then slightly later in the CNS, first in the brainstem solitary nucleus and subsequently in other brainstem nuclei (Table 1, Fig. 1, and Fig. S1), suggests that the A/Vietnam/1203/04 virus may enter the CNS via cranial nerves, as other strains of H5N1 are reported to do (17, 18). This hypothesis was tested by using microfluidic chambers that allow neuronal cell bodies and their processes to be grown in one compartment while their processes extend through 150-μm wide microgrooves into a separate process compartment (19). We added H5N1 virus to the process compartment for 1 h and detected virus in the cell bodies (Fig. 2*A*) and their processes (Fig. 2*B*) within the following 24 h. Because hydrostatic pressure differences between chambers would have confined extracellular virus to the process compartment, this finding showed that the virus detected in neuronal soma had been transported intracellularly. Direct exposure of cell bodies to H5N1 influenza also resulted in infection (Fig. 2*C*). These results demonstrate that H5N1 virus can infect neurons after peripheral infection and by hematogenous spread directly infecting cells as would occur after its release from dying cells.

One of the hallmarks of neurodegenerative disorders including Parkinson's and Alzheimer's disease is the aggregation of alpha-synuclein (20). This aggregation has been shown to depend on the phosphorylation of a number of serine residues in the synuclein protein (SYN), of which serine 129 appears to be most important (21). In 2–3-month-old uninfected C57BL/6J mice, we observed $_{P}$Ser129SYN in few, if any, neurons at any level of the central neuraxis, including the dopaminergic neurons of the substantia nigra pars compacta (Fig. 3*A*). However, in H5N1-infected mice, we observed $_{P}$Ser129SYN-positive neurons at various levels of the neuraxis including the brainstem and midbrain (Fig. 3*B*), hippocampus, and cortex. The phosphorylation of Ser129SYN appears to be directly related to H5N1 infection, because uninfected structures within the CNS did not show $_{P}$Ser129SYN up-regulation. Using NIH Image (version 1.63), we quantified the expression of p129SerSYN in olfactory bulb, hippocampus, locus coeruleus, brainstem and cerebellum. Animals infected with H5N1 infection had significantly increased expression of both cellular and secreted $_{P}$Ser129SYN at all levels of the neuraxis examined except for cerebellum (Table 2). In addition to $_{P}$Ser129SYN expression, we also noted aggregated alpha-synuclein in hippocampus (Fig. 3*C*), cortex, and brainstem, as seen in human proteinopathies such as Parkinson's and Alzheimer's diseases (20).

To determine whether H5N1 infection of the CNS resulted in cell death, we examined markers of apoptotic and necrotic cell death [caspase-3 activation (22) and Fluoro-Jade-B staining (23), respectively]. We also stereologically assessed dopaminergic neuron number in the substantia nigra pars compacta (SNpc). In regions of the brain where H5N1 virus had been detected, we found apoptotic (Fig. 3*D*) but not necrotic cells. We also noted activated microglia (Fig. 3*E*), which indicate an inflammatory process (24), in these regions. Microgliosis persisted in the CNS after the acute infection resolved and was observed during the entire 90-day study period (Fig. 3*F*). This prolonged inflammatory response is similar to that described in humans with idiopathic Parkinson's disease (25) and with parkinsonism induced by the neurotoxin MPTP (26). Cell counts of dopaminergic neurons in the SNpc 60 days after H5N1 infection demonstrated a 17% loss of dopaminergic neurons (8963 ± 384 DA neurons in control, 7481 ± 453 DA neurons in H5N1-infected mice, $n = 4$, $P \leq 0.016$).

Discussion

Reports of influenza-associated neurological syndromes are found as far back as 1385 and have continued through more recent influenza outbreaks (27). There is a substantial amount of evidence that influenza can directly lead to encephalitis (5, 28–33), although the link with development of neurodegenerative diseases including Parkinson's disease are controversial. Much of the linkage of parkinsonism with influenza infection are based on the postencephalic parkinsonism that followed an outbreak of von Economo's encephalopathy (EL) subsequent to the 1918 influenza pandemic (34). This includes epidemiological data (2, 3) and physical findings of type A influenza antigens in EL patients (35). Evidence against the role of influenza as a parkinsonian agent include the lack of viral RNA recovered from brains of postencephalic parkinsonian patients (36), the absence of any known mutations that

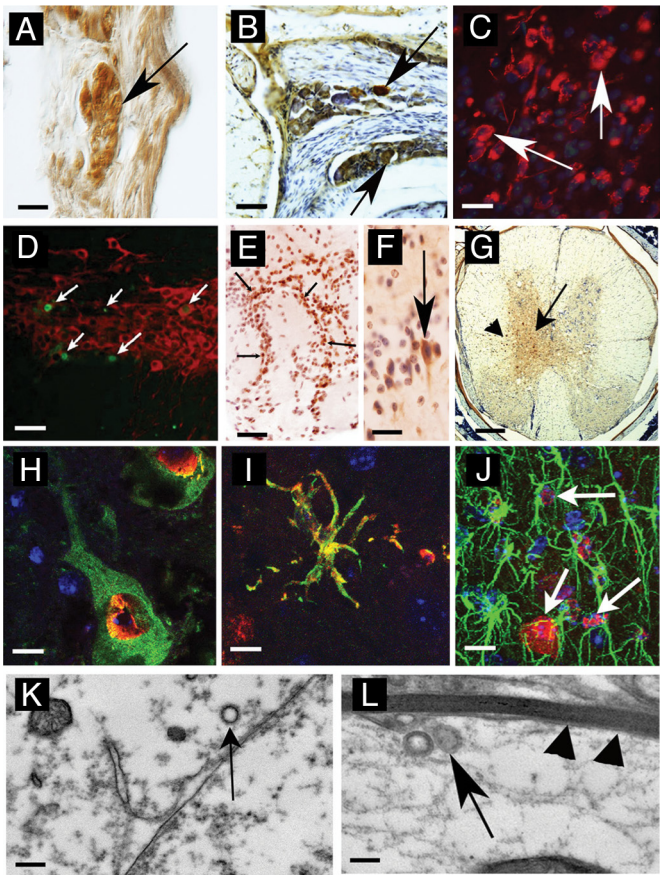

Fig. 1. Localization of A/Vietnam/1203/04 (H5N1) influenza virus in the nervous system. (*A*) Three days p.i. with H5N1, the virus is detected in Auerbach's plexus of the enteric nervous system (arrow) by using an antibody to the viral NP. (*B*) In the thoracic DRG, viral NP is first detected on day 3 p.i.; by day 10 p.i., virtually all large and medium-sized neurons (arrows), but few small neurons, are NP-positive. (*C*) At day 3 p.i., NP protein (red) is first detected in the neurons (white arrows) of the brainstem solitary nucleus. Blue stain is DAPI. (*D*) At day 7p.i., NP protein (green; arrows) is detected in the dopaminergic neurons of the SNpc (red, anti-TH). (*E* and *F*) At day 7 p.i., NP protein (brown) is found in the periglomerular cells (arrows, *E*) and mitral cells (arrow, *F*) of the olfactory bulb. (*G*) At day 10 p.i., NP protein is found in the spinal cord, primarily at the thoracic level. High levels of NP are seen around Clarke's column and the intermediomedial cell column (arrowhead). (*H*) NP protein (red) is found in the nuclei of neurons (blue, DAPI; green, anti-beta3-tubulin). (*I*) NP protein (red) is found in the nuclei and cytoplasm of microglia (blue, DAPI; green, anti-Iba-1; areas of colocalization are yellow). (*J*) NP protein (red; arrows) is not observed in astrocytes (green, anti-GFAP). (*K*) Transmission electron micrograph of a neuron in the brainstem shows a virus particle of the shape and size characteristic of influenza virus in the cytoplasm (arrow). The mitochondrion shows relative size. (*L*) Transmission electron micrograph of an axon traversing the brainstem shows virus particles of the characteristic shape and size of influenza virus in the axoplasm (arrow). Arrowheads indicate the myelin sheath surrounding the axon. [Scale bars: 20 μm (*A*);50 μm (*B*) ; 25 μm (*C*); 45 μm (*D*); 20 μm (*E*); 5 μm (*F*); 200 μm (*G*); 10 μm (*H*); 6 μm (*I*); 12 μm (*J*); 0.200 μm (*K*); 0.120 μm (*L*).]

would make the 1918 influenza virus neurotropic (34), and questions regarding the timeline of the 1918 pandemic waves and EL (37). Recently, Kobasa et al. administered the 1918 H1N1 influenza virus that was generated by plasmid-based reverse genetics and found no evidence of direct neurotropism (38). However, this engineered virus did induce a robust induction of cytokines including MCP-1, MIP-1beta, MIP-2, MIP-3alpha, IL-1beta, IL-6, IL-12 (p40), IL-18, and G-CSF (39), which can be secondarily activated in the brain without direct infection (40). Several of these cytokines have been implicated in the pathophysiology of Parkinson's disease (41).

In many cases of encephalitis and toxin-induced parkinsonism, the offending agent may cause a long lasting immune response in the brain that persists many years after the insult has resolved (26), leading to a "hit and run" mechanism where the original insult is no longer present but the secondary sequelae persists (42). This would fit our findings where we show the virus is gone from the brain in 21 days but there is a long-lasting activation of microglia and a significant loss of SNpc dopaminergic neurons. This "hit and run" mechanism would also be compatible with the absence of influenza viral RNA detection in archival brain tissue of postencephalic parkinsonian patients as reported by McCall et al. (36), because by the time the patient had passed away, the acute viral infection would have been resolved. Thus, if one accepts that influenza can activate the innate CNS immune system (43, 44) and induce a modest loss of neurons, there would be the necessity of a second hit that would lead to development of additional neuronal loss passing the threshold necessary for induction of parkinsonian symptoms (45) that would not have occurred without the priming that occurs via the influenza infection (46). In conclusion, we find that the highly infectious, neurotropic A/Vietnam/1203/04 (H5N1) influenza virus progresses from the peripheral nervous system into the CNS, where it activates the innate immune response in the brain. We have also shown that H5N1 influenza infection of the CNS can induce not only parkinsonian symptoms but also a significant increase in phosphorylation and aggregation of alpha synuclein, which likely results in the observed SNpc dopaminergic neuron degeneration (47). Thus, we suggest that any neurotopic influenza virus that activates the immune system in the brain could contribute to CNS disorders of protein aggregation (20, 48) and more generally that viruses may be an important etiological agent in the developmental sequalae of neurodegenerative diseases including Parkinson's disease.

Materials and Methods

All experimental infection of animals and handling of live H5N1 viruses were performed in a biosafety level 3+ laboratory approved for use by the U.S. Department of Agriculture and exclusively used by the Division of Virology and other approved scientists at St Jude Children's Research Hospital for highly pathogenic avian influenza work.

Virus Stock Preparation and Inoculation of Mice with H5N1. Stock viruses were prepared by propagating neurotropic A/Vietnam/1203/04 (H5N1) influenza virus for one passage in the allantoic cavity of 10-day-old embryonated chicken eggs for 40 to 48 h at 37 °C. Viral infectious titers were determined using the method of Reed and Muench (49), and expressed in $\log_{10}$ of the 50% egg infectious dose per 1.0 mL of fluid (EID_{50}/mL).

Six- to 8-week-old C57BL/6J mice (Jackson Labs) were anesthetized by Avertin and infected intranasally with 30 μL allantoic fluid diluted in PBS to the target virus infectious titer (10^2 EID_{50}).

Immunocytochemistry. Mice were anesthetized with Avertin at 1, 2, 3, 7, 10, 60, and 90 days after intranasal inoculation of H5N1 and transcardially perfused with 0.9% saline followed by 10% neutral buffered formalin. Brains and visceral organs were removed and postfixed for 3 weeks in 10% neutral buffered formalin to ensure that virus particles present in the tissue had been killed. The tissue was subsequently cryoprotected in 30% sucrose/PBS, serially sectioned at 20 μm, and mounted onto polyionic slides (Superfrost-plus, Fisher). H5N1 was detected with a pool of four monoclonal antibodies raised against the NP of influenza virus A/WSN/33 (H1N1) (50). The monoclonal antibodies target 4 different antigenic epitopes of the NP and detect all known subtypes of influenza A viruses. At least three different animals were used to determine the presence and distribution of H5N1 expression at each time point. H5N1 location was mapped using images generated from an electronic atlas (51), and a CNS nucleus template published in our lab (52). The volume of virus was scored in a semiquantitative manner that has been detailed (52).

Antibodies directed against GFAP were used to detect astrocytosis and antibodies directed against Iba-1 was used to detect microgliosis (53). Activated caspase-3 and Fluoro-Jade-B staining to mark apoptotic and necrotic

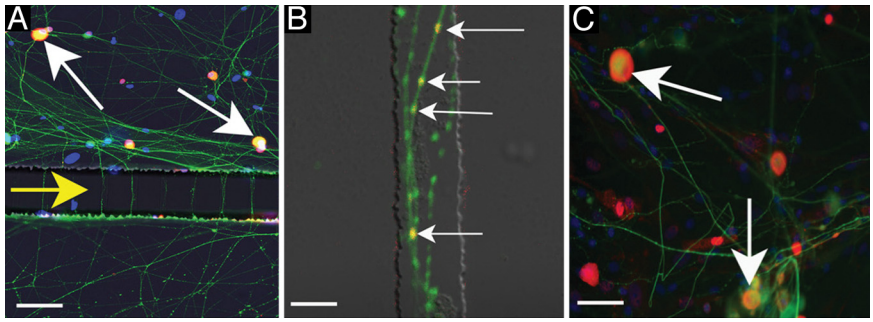

Fig. 2. Transport of H5N1 virus through axons in microfluidic chambers. (*A*) A/Vietnam/1203/04 (H5N1) influenza virus (2×10^6 PFU suspended in 20 μL serum-free medium) was added to the process compartments of microfluidic chambers containing freshly dissociated DRG (55). After 1 h, the process compartment was washed twice by adding 130 μL serum-free medium to the top reservoir and collecting the flow-through in the bottom reservoir. One hundred thirty microliters medium containing serum was then added to the top and bottom reservoirs of the process compartments to maintain hydrostatic balance. Twenty-four hours after addition of H5N1 virus to the process compartment (bottom), H5N1 NP is detected in neuronal bodies within the somal compartment (white arrows). Yellow arrow shows axons (green, beta3-tubulin) traversing the series of 150 μm-wide grooves between the compartments. (*B*) High power photomicrograph of DRG axons (green, beta3-tubulin) growing through the 150-μm grooves. Virus particles (arrows) within the axons appear yellow because of colocalization with neuronal beta3-tubulin. (*C*) Neuronal bodies (green) are infected after direct exposure to H5N1 virus (red, viral NP protein; arrows). Yellow indicates colocalization of proteins. [Scale bars: 160 μm (*A*); 6 μm (*B*); 60 μm (*C*).]

cells, respectively were examined as described in ref. 22. Alpha synuclein (BD Biosciences, cat# 610786) and pSER129 SYN (WAKO, monoclonal antibody #014–20281) immunocytochemistry were performed on frozen sections using standard protocols (53). Transmission electron microscopy was performed as described in ref. 54.

DRG Neuron Culture and Microfluidic Chamber Studies. Dissociated DRG neurons were prepared as described in ref. 55. Dissociated cells (60,000) were plated into the ''cell body compartment'' of microfluidic chambers (19). After 30 min to allow cell attachment, cultures were rinsed and 150 μL fresh media was added. At this time, 150 μL fresh medium containing 10 ng/mL nerve growth factor (NGF 2.5s, N6009, Sigma) was added to the ''process compartment'' of the microfluidic chamber. Cultures were incubated for 12 days at 5% CO_2, after which chambers were infected with 2×10^6 PFU of H5N1 in 20 μL media. After 1 h, the microfluidic axonal chamber was washed 2$\times$ by adding 130 μL serum free media to the top reservoir and collecting the flow through in the bottom reservoir. 130 μL media with serum was then added to the top and bottom reservoirs on the axonal side to maintain the hydrostatic balance. At the designated times, cells were rinsed with 1$\times$ PBS and fixed by 4% paraformadehyde for 1 h. Virus was detected by immunhistochemical methods as described above.

Quantification of the Phosphorylated α-Synuclein Expression. To ensure consistency in this analysis, all sections were processed on the same day using the same solutions and antibody preparations, including lot numbers. Sixteen-micrometer coronal frozen sections were washed with 0.1 M PBS. One set of section were incubated with 10 μg/mL proteinase K (Invitrogen)/0.1 M PBS solution for 10 min at room temperature, and another set of adjacent sections were washed with 0.1 M PBS without proteinase K. These different methods specifically allow identification of insoluble versus soluble pSer129SYN, respectively (56). All sections were blocked with M.O.M blocking solution (Vector Laboratories) for 1 h and incubated overnight at 4 °C with anti-phospho Ser129 antibody (1:1000, clone pSYN#64, WAKO) diluted in M.O.M diluent solution. Sections were incubated with a biotinylated secondary antibody for 30 min and then incubated with avidin-biotin complex (ABC kit, Vector Laboratories) for 15 min and washed in 0.1 M PBST 5$\times$ for 5 min each and developed with 3–3′ diaminobenzidine (Sigma) as the chromogen. Sections were dehydrated, cleared and mounted with Permount (Sigma). Images were captured at 10$\times$ using the virtual slice program in the Microbrightfield system (Microbrightfield) attached to an Olympus BX60 microscope. All images for analysis were taken at the same light intensity at one sitting to control for variations in bulb intensity and camera chip differences. All images were saved as a .tif file and optical densities of the rostral hippocampus, olfactory bulb, locus coeruleus, solitary nucleus, and cerebellum were obtained on raw

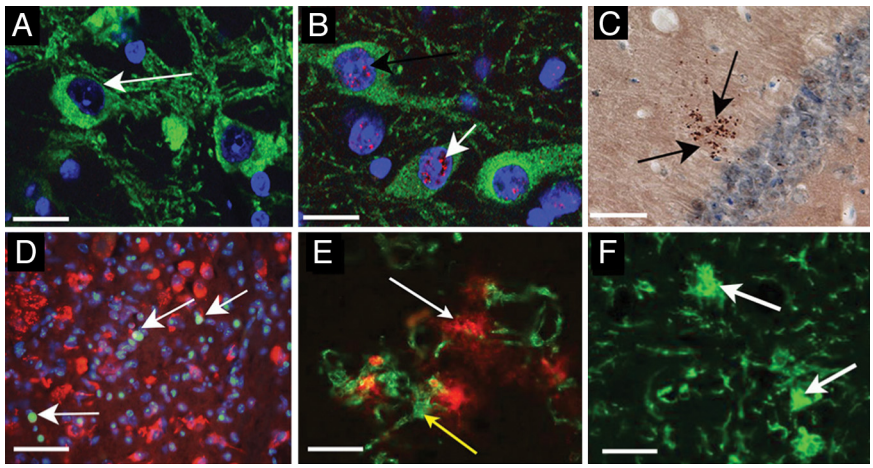

Fig. 3. A/Vietnam/1203/04 (H5N1) influenza virus induces a parkinsonian phenotype. (*A*) In uninfected C57BL/6J mice, no pSer129SYN is seen in the dopaminergic neurons of the SNpc (green). (*B*) At day 60 p.i., pSer129SYN (white arrows) is seen in the nuclei of dopaminergic neurons (green) in the SNpc. (blue, DAPI nuclear stain.) (*C*) At day 90 p.i., aggregated alpha synuclein (arrows) is seen in swollen neurites in the hippocampus. (*D*) At day 10 p.i., activated caspase-3 (arrows) is seen in brainstem regions that contain NP protein (red). The cells expressing activated caspase-3 do not appear to be NP-positive. (*E*) At day 10 p.i., activated microglia marked by anti-Iba-1 (green; yellow arrow) surround infected cells (red; white arrow). (*F*) At day 60 p.i., activated microglia (arrows) persist in midbrain regions (and all other regions) infected by H5N1. Findings were similar at day 90 p.i. [Scale bars: 30 μm (*A* and *B*); 50 μm (*C*); 40 μm (*D*); 35 μm (*E*); 50 μm (*F*).]

Table 2. Relative density measurements of pSer129SYN in brain

	no PK			pK-treated		
Structure	Control	H5N1	Statistics	Control	H5N1	Statistics
olfactory bulb	100 ± 19	178 ± 27	$P \leq 0.05$	100 ± 19	189.21 ± 23	$P \leq 0.01$
hippocampus	100 ± 21	277 ± 21	$P \leq 0.001$	100 ± 21	244 ± 25	$P \leq 0.001$
locus coeruleus	100 ± 20	120 ± 12	n.s.	100 ± 7	168 ± 10	$P \leq 0.001$
solitary nucleus	100 ± 18	190 ± 13	$P \leq 0.001$	100 ± 7	163 ± 8	$P \leq 0.001$
lower brainstem	100 ± 17	274 ± 37	$P \leq 0.001$	100 ± 21	135 ± 14	n.s.
cerebellum	100 ± 8	100 ± 3	n.s.	100 ± 16	108 ± 12	n.s.

Relative density measurements of p129SerSYN in brain. Both soluble p129SerSYN (noPK) and insoluble (pK) forms of this phosphoprotein were determined. Statistical analysis was performed using GraphPad software.

images using the NIH image program. The density of the background from each section was also obtained and subtracted from the region density to give a final number. Statistical analysis was performed using GraphPad statistical software.

Stereological Assessment of SNpc DA Neuron Number. SNpc dopamineric neurons were stereologically assessed using the optical fractionator as described in ref. 57.

ACKNOWLEDGMENTS. We thank Dr. Brian Davis for teaching DRG culture techniques and Sharon Naron for critical comments on the manuscript. This work was supported by National Institute of Allergy and Infectious Diseases Contract HHSN266200700005C (to R.W.), National Parkinson's Foundation (K.S.R. and R.J.S.), the Michael J. Fox Foundation (R.J.S.), National Institutes of Health Grant R21NS058310 (to R.J.S.), and the American Lebanese Syrian Associated Charities.

1. World Health Organization (2008) *Cumulative Number of Confirmed Human Cases of Avian Influenza A/(H5N1) Reported to WHO* (WHO, Geneva).
2. Maurizi CP (1985) Why was the 1918 influenza pandemic so lethal? The possible role of a neurovirulent neuraminidase. *Med Hypotheses* 16:1–5.
3. Ravenholt RT, Foege WH (1982) 1918 influenza, encephalitis lethargica, parkinsonism. *Lancet* 2:860–864.
4. Tanimura N, et al. (2006) Pathology of fatal highly pathogenic H5N1 avian influenza virus infection in large-billed crows (*Corvus macrorhynchos*) during the 2004 outbreak in Japan. *Vet Pathol* 43:500–509.
5. de Jong MD, et al. (2005) Fatal avian influenza A (H5N1) in a child presenting with diarrhea followed by coma. *N Engl J Med* 352:686–691.
6. Gambotto A, Barratt-Boyes SM, de Jong MD, Neumann G, Kawaoka Y (2008) Human infection with highly pathogenic H5N1 influenza virus. *Lancet* 371:1464–1475.
7. Mattson MP (2004) Infectious agents and age-related neurodegenerative disorders. *Ageing Res Rev* 3:105–120.
8. Reynolds A, Laurie C, Mosley RL, Gendelman HE (2007) Oxidative stress and the pathogenesis of neurodegenerative disorders. *Int Rev Neurobiol* 82:297–325.
9. Bertrand E, Lechowicz W, Szpak GM, Dymecki J (1997) Qualitative and quantitative analysis of locus coeruleus neurons in Parkinson's disease. *Folia Neuropathol* 35:80–86.
10. Gai WP, Blumbergs PC, Geffen LB, Blessing WW (1992) Age-related loss of dorsal vagal neurons in Parkinson's disease. *Neurology* 42:2106–2111.
11. Wakabayashi K, Takahashi H (1997) The intermediolateral nucleus and Clarke's column in Parkinson's disease. *Acta Neuropathol* 94:287–289.
12. Lewy F (1913) Zur pathologischen Anatomie der Paralysis agitans. *Deutsche Zeitschrift fur Nervenheilkunde* 50:50–55.
13. Duda JE, Lee VM, Trojanowski JQ (2000) Neuropathology of synuclein aggregates. *J Neurosci Res* 61:121–127.
14. Ilyushina NA, et al. (2008) Oseltamivir-ribavirin combination therapy for highly pathogenic H5N1 influenza virus infection in mice. *Antimicrob Agents Chemother* 52:3889–3897.
15. Hollis JH, Lightman SL, Lowry CA (2004) Integration of systemic and visceral sensory information by medullary catecholaminergic systems during peripheral inflammation. *Ann N Y Acad Sci* 1018:71–75.
16. Wood JM, Robertson JS (2004) From lethal virus to life-saving vaccine: Developing inactivated vaccines for pandemic influenza. *Nat Rev Microbiol* 2:842–847.
17. Iwasaki T, et al. (2004) Productive infection in the murine central nervous system with avian influenza virus A (H5N1) after intranasal inoculation. *Acta Neuropathol (Berl)* 108:485–492.
18. Tanaka H, et al. (2003) Neurotropism of the 1997 Hong Kong H5N1 influenza virus in mice. *Vet Microbiol* 95:1–13.
19. Liu WW, Goodhouse J, Jeon NL, Enquist LW (2008) A microfluidic chamber for analysis of neuron-to-cell spread and axonal transport of an alpha-herpesvirus. *PLoS ONE* 3:e2382.
20. Jellinger KA (2008) Neuropathological aspects of Alzheimer disease, Parkinson disease and frontotemporal dementia. *Neurodegener Dis* 5:118–121.
21. Anderson JP, et al. (2006) Phosphorylation of Ser-129 is the dominant pathological modification of alpha-synuclein in familial and sporadic Lewy body disease. *J Biol Chem* 281:29739–29752.
22. Faherty CJ, Xanthoudakis S, Smeyne RJ (1999) Caspase-3-dependent neuronal death in the hippocampus following kainic acid treatment. *Mol Brain Res* 70:159–163.
23. Schmued LC, Hopkins KJ (2000) Fluoro-Jade: Novel fluorochromes for detecting toxicant-induced neuronal degeneration. *Toxicologic Pathology* 28:91–99.
24. Liu B, Hong JS (2003) Role of microglia in inflammation-mediated neurodegenerative diseases: Mechanisms and strategies for therapeutic intervention. *J Pharmacol Exp Ther* 304:1–7.
25. Mosley RL, et al. (2006) Neuroinflammation, oxidative stress and the pathogenesis of Parkinson's disease. *Clin Neurosci Res* 6:261–281.
26. Langston JW, et al. (1999) Evidence of active nerve cell degeneration in the substantia nigra of humans years after 1-methyl-4-phenyl-1,2,3,6-tetrahydropyridine exposure. *Ann Neurol* 46:598–605.
27. Jang H, Boltz DA, Webster RG, Smeyne RJ (2008) Viral parkinsonism. *Biochim Biophys Acta* 1792:714–721.
28. Hayase Y, Tobita K (1997) Influenza virus and neurological diseases. *Psychiatry Clin Neurosci* 51:181–184.
29. Drago L, Attia MW, DePiero A, Bean C (2005) Influenza A-associated meningoencephalitis. *Pediatr Emerg Care* 21:437–439.
30. Togashi T, Matsuzono Y, Narita M, Morishima T (2004) Influenza-associated acute encephalopathy in Japanese children in 1994–2002. *Virus Res* 103:75–78.
31. Iijima H, Wakasugi K, Ayabe M, Shoji H, Abe T (2002) A case of adult influenza A virus-associated encephalitis: Magnetic resonance imaging findings. *J Neuroimaging* 12:273–275.
32. Mihara M, Utsugisawa K, Konno S, Tohgi H (2001) Isolated lesions limited to the bilateral substantia nigra on MRI associated with influenza A infection. *Eur Neurol* 45:290–291.
33. Lawrence GH, Jones RA (1957) Case report: Encephalitis as a complication of the influenza. *Mo Med* 54:1164 passim.
34. Taubenberger JK (2006) The origin and virulence of the 1918 ''Spanish'' influenza virus. *Proc Am Philos Soc* 150:86–112.
35. Gamboa ET, et al. (1974) Influenza virus antigen in postencephalitic parkinsonism brain. Detection by immunofluorescence. *Arch Neurol* 31:228–232.
36. McCall S, Henry JM, Reid AH, Taubenberger JK (2001) Influenza RNA not detected in archival brain tissues from acute encephalitis lethargica cases or in postencephalitic Parkinson cases. *J Neuropathol Exp Neurol* 60:696–704.
37. Casals J, Elizan TS, Yahr MD (1998) Postencephalitic parkinsonism–a review. *J Neural Transm* 105:645–676.
38. Kobasa D, et al. (2007) Aberrant innate immune response in lethal infection of macaques with the 1918 influenza virus. *Nature* 445:319–323.
39. Kobasa D, et al. (2004) Enhanced virulence of influenza A viruses with the haemagglutinin of the 1918 pandemic virus. *Nature* 431:703–707.
40. Hansen MK, et al. (2000) Effects of vagotomy on lipopolysaccharide-induced brain interleukin-1beta protein in rats. *Auton Neurosci* 85:119–126.
41. Koprich JB, Reske-Nielsen C, Mithal P, Isacson O (2008) Neuroinflammation mediated by IL-1beta increases susceptibility of dopamine neurons to degeneration in an animal model of Parkinson's disease. *J Neuroinflammation* 5:8.
42. Tansey MG, McCoy MK, Frank-Cannon TC (2007) Neuroinflammatory mechanisms in Parkinson's disease: Potential environmental triggers, pathways, and targets for early therapeutic intervention. *Exp Neurol* 208:1–25.
43. Mori I, Imai Y, Kohsaka S, Kimura Y (2000) Upregulated expression of Iba1 molecules in the central nervous system of mice in response to neurovirulent influenza A virus infection. *Microbiol Immunol* 44:729–735.
44. Dhib-Jalbut S, Gogate N, Jiang H, Eisenberg H, Bergey G (1996) Human microglia activate lymphoproliferative responses to recall viral antigens. *J Neuroimmunol* 65:67–73.
45. Weidong L, Shen C, Jankovic J (2009) Etiopathogenesis of Parkinson disease: A new beginning? *Neuroscientist* 15:28–35.
46. Peng J, Peng L, Stevenson FF, Doctrow SR, Andersen JK (2007) Iron and paraquat as synergistic environmental risk factors in sporadic Parkinson's disease accelerate age-related neurodegeneration. *J Neurosci* 27:6914–6922.
47. Gao HM, et al. (2008) Neuroinflammation and oxidation/nitration of alpha-synuclein linked to dopaminergic neurodegeneration. *J Neurosci* 28:7687–7698.
48. Tansey MG, et al. (2008) Neuroinflammation in Parkinson's disease: Is there sufficient evidence for mechanism-based interventional therapy? *Front Biosci* 13:709–717.
49. Reed LJ, Muench H (1938) A simple method of estimating 50 percent end-points. *Amer J Hygiene* 27:493–497.

50. van Wyke KL, Hinshaw VS, Bean WJ, Jr, Webster RG (1980) Antigenic variation of influenza A virus nucleoprotein detected with monoclonal antibodies. *J Virol* 35:24–30.
51. Paxinos G, Franklin KBJ (2001) in *The Mouse Brain in Stereotaxic Coordinates* (Academic, San Diego).
52. Chen SC, Kochan JP, Campfield LA, Burn P, Smeyne RJ (1999) Splice variants of the OB receptor gene are differentially expressed in brain and peripheral tissues of mice. *J Recept Signal Transduct Res* 19:245–266.
53. Smeyne M, Jiao Y, Shepherd KR, Smeyne RJ (2005) Glia cell number modulates sensitivity to MPTP in mice. *Glia* 52:144–152.
54. Ajioka I, et al. (2007) Differentiated horizontal interneurons clonally expand to form metastatic retinoblastoma in mice. *Cell* 131:378–390.
55. Malin SA, Davis BM, Molliver DC (2007) Production of dissociated sensory neuron cultures and considerations for their use in studying neuronal function and plasticity. *Nat Protoc* 2:152–160.
56. Fleming SM, et al. (2008) Olfactory deficits in mice overexpressing human wildtype alpha-synuclein. *Eur J Neurosci* 28:247–256.
57. Baquet ZC, Williams D, Brody J, Smeyne RJ (2009) A comparison of model-based (2D) and design-based (3D) stereological methods for estimating cell number in the substantia nigra pars compacta (SNpc) of the C57BL/6J Mouse. *Neuroscience.*